Increased surface plasmon resonance sensitivity with the use of double Fourier harmonic gratings

Nicolas Bonod[1], Evgeny Popov[1], Ross C. McPhedran[2]

[1]*Institut Fresnel, CNRS UMR 6133, Aix-Marseille Université, Domaine Universitaire de Saint Jérôme, 13397 Marseille Cedex 20, FRANCE*

[2]*CUDOS School of physics, University of Sydney, New South Wales 2006, Australia*

[*]*Corresponding author: nicolas.bonod@fresnel.fr*

Abstract: A biomolecular sensor consisting of a thin metallic grating deposited on a glass prism is studied in the formalism of poles and zeros of the scattering matrix. Surface plasmon resonance is used to increase the sensitivity of the device with respect to a variation of the refractive index of the substrate. It is shown that a direct coupling between counter propagating surface plasmons using double-harmonic Fourier gratings leads to an enhancement of the sensitivity. The result of the stronger coupling is the transfer of the working point from the lower to the upper edge of the band gap in the dispersion diagram.

©2008 Optical Society of America

OCIS codes: (240.6680) Surface Plasmons; (130.6010) Sensors; (050.1950) Diffraction gratings.

References and links

1. E. Kretschmann, "Determination of optical constants of metals by excitation of surface Plasmons," Z. Phys. **241**, 313- (1971).
2. R. W. Wood, "On a remarkable case of uneven distribution of light in a diffraction grating spectrum," Philos. Mag. **4**, 396-402 (1902)
3. J. J. Cowan and E. T. Arakawa, "Dispersion of surface plasmons in dielectric-metal coatings on concave diffraction gratings," Z. Phys. **235**, 97- (1970).
4. D. Maystre and R.C. McPhedran, "A detailed theoretical study of the anomalies of a sinusoidal diffraction grating," Optica Acta **21**, 413-421 (1974).
5. M. Neviere, "The homogeneous problem," in *Electromagnetic theory of gratings*, R. Petit ed. (Springer-Verlag, 1980), ch.5
6. H. Raether, *Surface Plasmons on Smooth and Rough Surfaces and on Gratings* (Springer-Verlag, Berlin, 1988)
7. M. J. Jory, P. S. Vukusic, and J. R. Sambles, "Development of a prototype gas sensor using surface plasmon resonance on gratings," Sens. Actuators B **17,** 203-209 (1994).
8. U. Schroter and D. Heitmann, "Grating couplers for surface plasmons excited on thin metal films in the Kretschmann-Raether configuration," Phys. Rev. B **60,** 4992-4999 (1999).
9. J. Homola, S. S. Yee and G. Gauglitz, "Surface plasmon resonance sensors: review," Sens. Act. B **54**, 3-15 (1999)
10. F. Pigeon, I. F. Salakhutdinov, A. V. Tishchenko, "Identity of long-range surface plasmons along asymetric structures and their potential for refractometric sensors," J. Appl. Phys. **90**, 852-859 (2001)
11. C. J. Alleyne, A.G. Kirk, R. C. McPhedran, N-A. P. Nicorovici and D. Maystre, "Enhanced SPR sensitivity using periodic metallic structures," Opt. Express **15**, 8163-8169 (2007).
12. D. Maystre, "General study of grating anomalies from electromagnetic surface modes", in *Electromagnetic Surface Modes*, A.D. Boardman, ed. (John Wiley, 1982), Chap. 17.
13. M. Breidne and D. Maystre, "A systematic numerical study of Fourier gratings", J. Opt. **13**, 71-79 (1982).
14. J. Chandezon, D. Maystre and G. Raoult, "A new theoretical method for diffraction gratings and its numerical application," J.Opt. **11**, 235-241 (1980).
15. L. Li, "Oblique-coordinate-system-based Chandezon method for modeling one-dimensionally periodic, multilayer, inhomogeneous, anisotropic gratings," J. Opt. Soc. Am. **16**, 2521-2531 (1999).
16. D. Maystre and R. Petit, "Brewster incidence for metallic gratings," Opt. Commun. **17**, 196-200 (1976).
17. M. C. Hutley and D. Maystre, "The total absorption of light by a diffraction grating," Opt. Commun. **19**, 431-436 (1976)

#96429 - $15.00 USD Received 20 May 2008; revised 14 Jul 2008; accepted 16 Jul 2008; published 21 Jul 2008

(C) 2008 OSA

18. M. D. Malinsky, K. L. Kelly, G. C. Schatz, and R. P. Van Duyne, "Chain Length Dependence and Sensing Capabilities of the Localized Surface Plasmon Resonance of Silver Nanoparticles Chemically Modified with Alkanethiol Self-Assembled Monolayers," J. Am. Chem. Soc. **123,** 1471-1482 (2001).

1. Introduction

The technique of surface plasmon resonance has found wide use in recent years in biosensing applications, with the principal configuration employing a prism in the frustrated or attenuated total reflection configuration associated with the name of Kretschmann [1]. Another convenient method for exciting surface plasmons for use in sensing is to employ surface relief gratings, which since the early years of the last century have been known to exhibit diffraction anomalies [2] sensitive to surface conditions on the grating. The connection between Wood anomalies and surface plasmons was established decisively by Cowan and Arakawa [3], and since then the plasmon effect on gratings has been used both as a sensitive test of the accuracy of diffraction grating theories [4,5] and in sensing applications [6-9].

Surface Plasmons Polaritons (SPP) induce a strong enhancement of the electromagnetic field at the interface between metal and dielectric. As a consequence, they are widely used in the optical sensing of molecules or virus adsorbed by the interface or diffusing on the substrate. Biosensors based on SPP are highly dependent on the refractive index of the surrounding media. Binding, adsorbtion of molecules on the metallic surface, induces a change of the local refractive index of the dielectric medium, so that such biosensors can be called refractometric sensors [10]. Localized plasmons can be considered when using metallic nanospheres, and delocalized plasmons can be considered when using a flat metallic interface. SPP on a flat interface are often excited in the Kretschmann configuration. A thin metallic layer is coated on a glass slide, and SPP can propagate along the interface between the metal and the superstrate, made of air or water for example. In this case, the interaction between SPP at both interfaces can split the dispersion curves of SPP and long range surface plasmon polaritons (LRSPP) characterized by very low propagation losses can be excited. LRSPP are symmetric or asymmetric when both embedding media are respectively identical or different. In 2001, F. Pigeon et al. [10] demonstrated that asymmetric LRSPP present a low refractometric sensitivty compared with standard SPP.

In this study, we consider standard SPP excited at the interface between metal and substrate. A recent study [11] has shown that by placing a sinusoidal profile grating in silver of appropriate period and depth on the rear face of a substrate used in the Kretschmann configuration, the surface plasmon resonance (SPR) sensitivity may be enhanced by a factor of six when compared with an uncorrugated surface. Here we will analyze this result in terms of the poles of the scattering matrix associated with surface plasmons, and the associated zeros, and will explain the enhanced sensitivity of the optimal configuration in terms of the relative trajectory of poles and zeros as a function of grating depth. (For a review of the connection between anomalies, poles, zeros and surface modes, see the chapter by D. Maystre [12]). We will go further by considering the enlarged parameter space arising when instead of a simple sinusoidal grating we consider a grating whose profile is composed of two Fourier harmonics. We will show that such compound profile gratings can provide a further sixty percent increase in plasmon resonance sensitivity above that provided by the sinusoidal profile, and that this heightened sensitivity is achieved because the operating point of the sensor moves from the lower frequency edge of a minigap between two plasmon dispersion curves to the upper frequency edge.

It should be stressed that gratings with profiles composed of superposed Fourier harmonics can be created by established interference techniques [13]. Although their fabrication offers an additional degree of complexity, they do offer the advantages of relatively large area grating format, possibility of mosaic gratings on a single substrate and precision replication through several generations from a single master in common with sinusoidal and ruled gratings. These advantages mean that such interference gratings are not incompatible with fabrication of relatively low-cost, high sensitivity surface plasmon sensors.

#96429 - $15.00 USD Received 20 May 2008; revised 14 Jul 2008; accepted 16 Jul 2008; published 21 Jul 2008
(C) 2008 OSA

In the next section, we consider the case of a sinusoidal grating used as an SPR sensor, and show how the optimization of its sensitivity may be achieved simply by regarding the behaviour of the trajectories of the zeros and poles of the scattering matrix. We use this insight in Section 3, where we study the case of a Fourier grating with two superposed surface modulations. We show that this design yields a 60% enhancement in sensitivity compared with the sinusoidal case, and further that the reflectance minimum now is a single feature rather than a double dip, a simplifying feature for automated SPR analysis. In Section 4 we give dispersion diagrams, which show that the improved sensitivity of the Fourier grating is the result of the operating point moving from the lower frequency side of a photonic minigap to the upper, flatter side. Section 5 contains our concluding remarks.

2. Single harmonic Fourier grating

The periodic metallic film under study is depicted in Fig.1. The substrate is water (refractive index n_1=1.33), the superstrate is glass (n_3=1.5). The thickness of the metallic layer is taken to be 40 nm. The period of the grating is 0.3 μm. It is illuminated from the glass by a plane wave in Transverse Magnetic polarization (TM), with angle of incidence θ. In this way, it is possible to excite from the 0th order a surface plasmon resonance at the water-metal interface when the condition $\alpha_i \equiv n_3 \sin\theta = \alpha_{spp1\text{-}2}$ is satisfied, where $\alpha_{spp1\text{-}2}$ is the normalized propagating constant of the surface plasmon. This surface plasmon will propagate in the Ox direction. It is possible to excite simultaneously from the -1st order a surface plasmon propagating along both metallic interfaces in the –Ox direction when the two equalities: $n_3 \sin\theta - \lambda/d = -\alpha_{spp1\text{-}2}$ and $n_3 \sin\theta - \lambda/d = -\alpha_{spp3\text{-}2}$ are satisfied. These surface plasmons propagate on the lower and upper metallic interfaces respectively. The surface plasmon $\alpha_{spp3\text{-}2}$ propagating on the interface between prism and metal will not be modified by a slight variation of the refractive index n_1 of the water and is not of interest in this study.

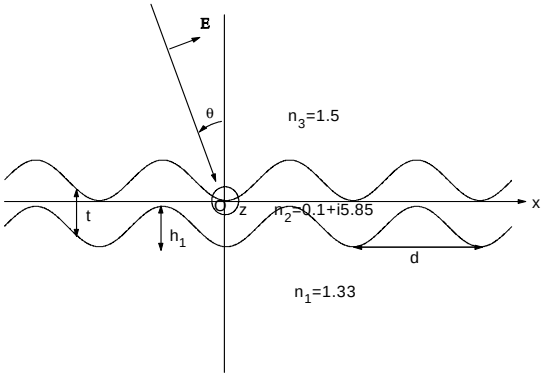

Fig. 1. Periodically corrugated prism of refractive index n_3 = 1.5 coated by a metallic layer of thickness t (t=40 nm) and refractive index equal to 0.1 + i 5.85, corresponding to silver at a wavelength of 850 nm. Grooves have a sinusoidal geometry with height h_1 and period d. The substrate is made of water with refractive index n_1 = 1.33 or 1.34.

The diffraction problem is numerically solved by the use of the profile transformation method due to Chandezon et al. [14, 15]. The scattering matrix S is defined as $S(\alpha)\, I = D$, where I and D represent column vectors made of the Fourier components of the x and z components of the incident (I) and diffracted (D) electric and magnetic fields. The complex solutions α_p denoting poles are the solutions of the homogeneous problem:

$$S^{-1}(\alpha_p)\, D = 0, \qquad (1)$$

#96429 - $15.00 USD Received 20 May 2008; revised 14 Jul 2008; accepted 16 Jul 2008; published 21 Jul 2008
(C) 2008 OSA

whereas α_z represents a zero of the 0th reflected order:

$$S_{0,0}(\alpha_z) = 0. \quad (2)$$

The complex propagation constant of a surface plasmon α_{spp} satisfies Eq. (1) and is identified with α_p. When considering perfectly conducting metals, $\alpha_z = \alpha_p^*$ [10], where the asterisk stands for the complex conjugate. With finite conductivity metals, it has been shown that the trajectory of the zero when varying the groove depth is almost symmetric to that of the pole with respect to the unperturbed trajectory (that of a perfectly conducting grating) [10]. The real part of the zero indicates a minimum of the reflected efficiency when varying the x component of the incident wavevector $\alpha_i = n_3 \sin\theta$. If the imaginary part of the zero is zero, then the reflected efficiency will be equal to zero.

We study the poles α_p corresponding to the two counter propagating surface plasmons at the water-metal interface as a function of h_1 for the refractive indices $n_1 = 1.33$ and 1.34 (water and water infused with a biomolecule). The two counter propagating surface plasmons excited by the 0th and the –1st orders present two different values of α_p, in full and dashed lines in Fig. 2, since two different equations must be satisfied, respectively:

$$\alpha_p - \lambda / d = -\alpha_{spp1\text{-}2} \quad (3)$$

and

$$\alpha_p = \alpha_{spp1\text{-}2} \quad (4)$$

The surface plasmon excited by the –1st order propagates along the –Ox direction and has a propagation constant with a negative imaginary part (the full line in Fig. 2). In order to distinguish in another way the two surface plasmons in Fig. 2, we note that when the groove depth increases, the propagation of the surface plasmon is perturbed, as it radiates more strongly in the prism. As a consequence, the real part of $\alpha_{spp1\text{-}2}$ increases. α_p must be decreased to fulfill Eq. (3) and must be increased to fulfill Eq. (4). As a result, the full lines and dashed lines in Fig. 2 that represent respectively the propagation constant of the surface plasmons excited by the –1st and the 0th orders approach each other when increasing the groove depth.

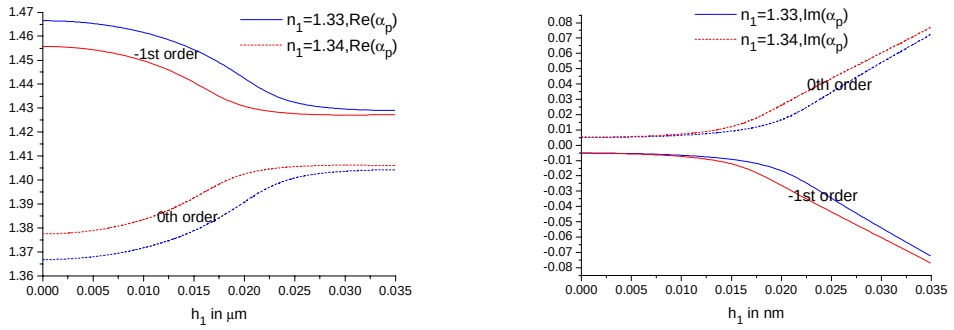

Fig. 2. Real (a) and imaginary parts (b) of the poles satisfying eq.(1) as a function of h_1, for two refractive indices of the substrate 1.33 (blue) and 1.34 (red). Dashed line: surface plasmon excited by the 0th order, full line surface plasmon excited by the –1st order.

The zeros corresponding to the poles in Fig. 2 are displayed in Fig. 3. It can be observed that by contrast with what happens with the poles, the imaginary part of the zero can vanish (see the dashed line in Fig. 3(b), which will correspond to a zero of the reflectivity of the device [12]. Excitation of a surface plasmon by the 0th order is responsible for the full absorption of incident light by the grating [16, 17].

#96429 - $15.00 USD Received 20 May 2008; revised 14 Jul 2008; accepted 16 Jul 2008; published 21 Jul 2008
(C) 2008 OSA

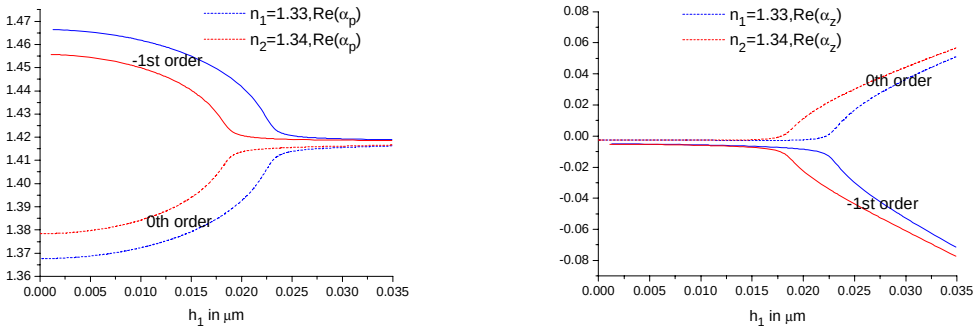

(a) (b)

Fig. 3. Similar to Fig. 2 with the zeros satisfying Eq.(2).

Now, we are interested in the increase of the sensitivity of the surface plasmons with the change of the refractive index n_1 of the substrate. The difference between real parts in Fig. 3(a) has to be maximized, while the imaginary part of α_z has to be minimized. When increasing h_1, the coupling between the two counter propagating surface plasmons increases. As a result, the constants of propagation tend toward the same value, with an increase of the imaginary part.

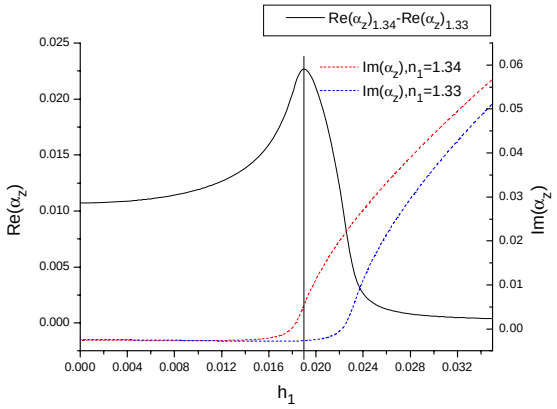

Fig. 4. Difference between the real parts of the zeros with refractive index of 1.34 and 1.33 as a function of h_1 (full black curve with the right scale) with imaginary parts of the zeros associated with the surface plasmon excited by the 0th order (dashed lines with the left scale).

#96429 - $15.00 USD Received 20 May 2008; revised 14 Jul 2008; accepted 16 Jul 2008; published 21 Jul 2008
(C) 2008 OSA

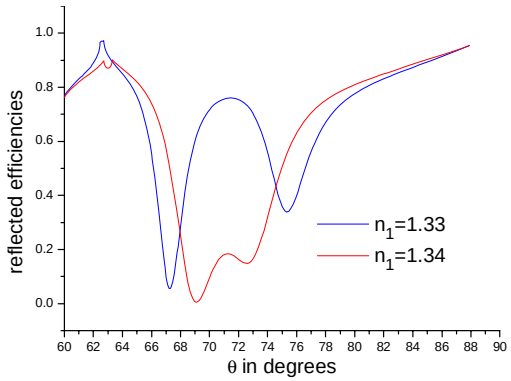

Fig. 5.Reflected efficiency as a function of the angle of incidence θ, with h_1=0.017 μm.

The maximum of the shift between red and blue curves will occur when the real part of surface plasmon for n_1 = 1.34 stops to increase further when increasing h_1, in other words when the imaginary part becomes important for n_1 = 1.34 and still negligible for n_1=1.33, which happens around h_1 = 20 nm. Figure 4 shows the difference between the blue and red dashed lines of Fig. 3a as a function of h_1, together with the imaginary parts of α_z. The sensitivity of the propagation constant of the surface plasmon with the refractive index n_1 is maximal for h_1 = 0.019 μm. However, the imaginary part of α_z with n_1 = 1.34 is too high so that the minimum of reflectivity will not be pronounced, and the width at mid-height will be too large. As a consequence, h_1 = 0.017 μm is preferable for the plot of the reflectivity as a function of the angle of incidence (Fig. 5). The two minima of reflectivity obtained with n_1=1.33 and 1.34 are separated by Δθ = 6.25° (using the leftmost dip for n = 1.33 and the rightmost dip for n = 1.34).

3. Double Fourier harmonic grating

With the aim of improving the coupling between the two counter propagating surface plasmons, a second periodic modulation is added (Fig. 6), with a groove height h_2. The profile represents a function with equation: $h_1 \sin(\frac{2\pi}{d}x) + h_2 \sin(\frac{4\pi}{d}x + \varphi)$.

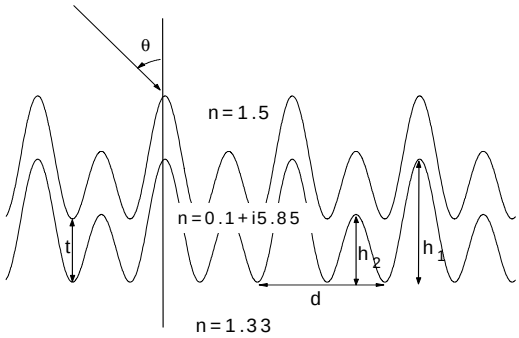

Fig. 6. Same as Fig. 1 with a second periodical modulation of height h_2.

#96429 - $15.00 USD Received 20 May 2008; revised 14 Jul 2008; accepted 16 Jul 2008; published 21 Jul 2008
(C) 2008 OSA

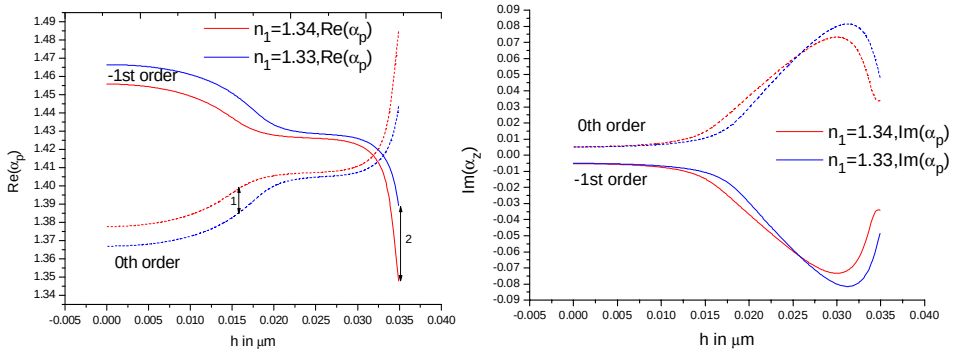

Fig. 7. Real (a) and imaginary parts (b) of the zeros satisfying eq.(2) as a function of h_1, for two refractive index of the substrate 1.33 (blue) and 1.34 (red). Dashed line: surface plasmon excited by the 0th order, full line surface plasmon excited by the –1st order. t = 40 nm and $\varphi = \pi/2$.

A full numerical optimization as a function of d, t, φ, h_1 and h_2 has been computed in order to obtain the largest variation of the absorption as a function of θ associated with a very low reflectivity, close to zero. As a result of this, the values h_1 = 35 nm, h_2 = 59 nm, t = 40 nm and $\varphi = \pi/2$ have been selected. In order to understand why the second modulation permits an enhanced SPR sensitivity, the poles are plotted as a function of the groove depth h defined by the groove geometry (Fig. 6):

$$h\left(\sin(\frac{2\pi}{d}x)+\frac{59}{35}\sin(\frac{4\pi}{d}x-\frac{\pi}{2})\right). \qquad (5)$$

For shallow grooves (h < 25 nm), the trajectory of the poles in the complex plane as a function of h is similar to that obtained with the single Fourier harmonic grating. The sensitivity is maximum around h = 15 nm (first double arrow in Fig. 7a). The imaginary parts are maximal in magnitude when the real parts cross, due to the strong coupling of the two counter propagating surface plasmons. This region is known as a band gap occurring at the borders of the Brillouin zone, as discussed in the next section. Further increase of the groove depth causes the propagation constant of the surface plasmon excited by the 0th order to become higher than that of the plasmon excited by the –1st order, which decreases their coupling and subsequently permits us to decrease the imaginary part of the propagation constant of the surface plasmons (Fig. 7b) and to significantly increase the separation between the real parts (right-side double arrow in Fig. 7a). The sensitivity of the propagation constant of surface plasmons with respect to n_1 is then at a maximum.

#96429 - $15.00 USD Received 20 May 2008; revised 14 Jul 2008; accepted 16 Jul 2008; published 21 Jul 2008
(C) 2008 OSA

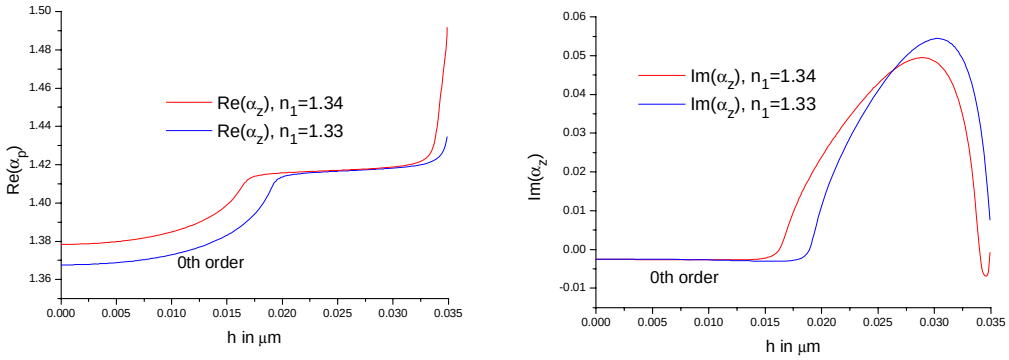

(a) (b)

Fig. 8. Real (a) and imaginary parts (b) of the zeros satisfying eq.(2) as a function of h, for two refractive indices of the substrate: 1.33 (blue) and 1.34 (red). Zeros are associated with the surface plasmon excited by the 0th order. t=40 nm and $\varphi=\pi/2$.

The trajectory of the zero associated with the pole plotted in Fig. 7 (dashed line) is displayed in Fig. 8. The zero associated with the other surface plasmon will present too large an imaginary part and will not contribute to the full absorption of incident light. This confirms the explanation given with the poles: when h=35 nm, the sensitivity of the real part to n_1 is maximal and imaginary parts are minimized. As a consequence, in the plot of the reflectivity of the device as a function of the angle of incidence with h=35 nm (Fig. 9), the minima are well pronounced and very close to zero, and they are very well separated, with a variation of $\Delta\theta = 10°$ with $\Delta n = 0.01$.

The study of the device sensitivity has two aspects, which depend on its use. The first possibility is to monitor the reflectivity at a given angle of incidence θ. The influence of the variation of the refractive index of the substrate n by one part in a thousand on the reflectivity R for two different values of θ is presented in Fig. 10a. The sensitivity varies between 2% and 10% per 0.001 Δn, depending on the value of n and θ. The second possibility is to monitor the incident angle θ_{min} corresponding to the minimum reflectivity. This can be made by using a diverging incident beam and measuring a response using CCD camera. The sensitivity varies between 0.7 and 1.4 degree per 0.001 Δn, as observed in Fig. 10(b).

We can put the sensitivity curves of Fig. 10 into context by comparing them with the results in the experimental study of surface plasmon sensors using silver nanoparticle arrays by Malinsky et al [18]. They studied alkanethiol self-assembled monolayers on the silver nanoparticles, and in particular 1-HDT (1-Hexadecanethiol). Their detection limit using LSPR (localized surface plasmon resonance) was 2-3% of a monolayer of 1-HDT on a single nanoparticle, and they were able to show that the maximum absorption wavelength of the LSPR shifted to the red by 3 nm for every extra carbon in the alkane chain, due to the increased thickness of the adsorbed layer. Using their value for the dielectric constant (2.10) of a self-assembled monolayer of 1-HDT, we can estimate the volume fraction of 1-HDT required for a refractive index change of one part in a thousand to be 0.8%, so that the sensitivities displayed in Fig. 10 are of the same magnitude as those demonstrated by Malinsky et al [18]. The wavelength resolution corresponding to the angular resolution in Fig. 10 b is sufficient to resolve the shift of 3 nm per extra carbon atom in the alkane chain, again corroborating the conclusion that the double Fourier grating design delivers sufficient sensitivity for practical applications in molecular spectroscopy.

As can be expected, the high sensitivity of the device imposes tight tolerances on the grating parameters. For example, increase of the total groove depth by 5% shifts the position of the reflectivity minima by about 3°, as observed in Fig. 11(a). In addition, in order to obtained a performance similar to Fig. 9, it is also necessary to increase the metallic layer

#96429 - $15.00 USD Received 20 May 2008; revised 14 Jul 2008; accepted 16 Jul 2008; published 21 Jul 2008
(C) 2008 OSA

thickness. Although such error reduces the working interval on n, the sensitivity of the device remains the same as for the original profile having optimal groove depth, as can be observed in Fig. 11(b).

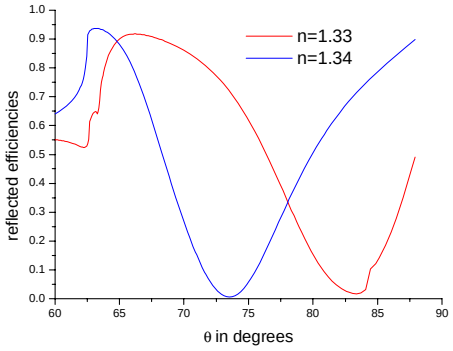

Fig. 9. Reflected efficiency as a function of the angle of incidence θ. h_1=35 nm, h_2 = 59 nm, t = 40 nm, φ=π/2.

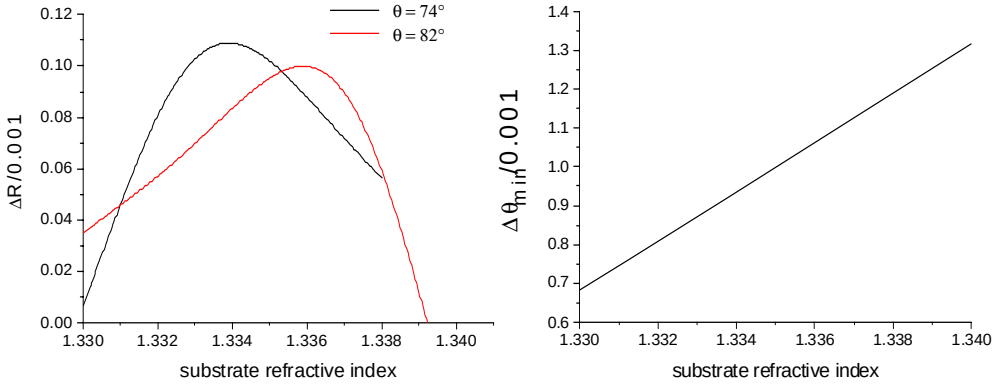

(a) (b)

Fig. 10. Sensitivity of the device per Δn = 1/1000. (a) Change of the reflectivity R at a fixed angle of incidence (the values given in the insert). (b) Change in the incident angle corresponding to the minimum of reflectivity

#96429 - $15.00 USD Received 20 May 2008; revised 14 Jul 2008; accepted 16 Jul 2008; published 21 Jul 2008
(C) 2008 OSA

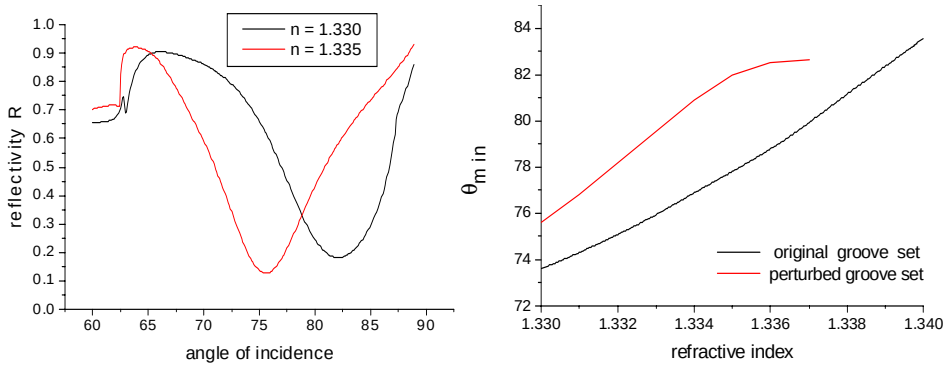

(a) (b)

Fig. 11. Variation of the device performance with 5% error in the groove height. (a) Same as in Fig.9 but for h increased by 5% and t = 50 nm. (b) Position of the angle of minimum reflectivity for the original groove profile (h = 35 nm) and for the profile with h increased by 5% and t = 50 nm

4. Dispersion diagrams

In order to better understand the difference between the single- and the double-harmonic gratings, in this section we present the ω-k diagrams, which show the formation of an ω-gap and its link with the poles of the scattering matrix, discussed in the previous sections. Figure 12a presents the map of the intensity of the 0th reflected order as a function of k_x and ω/c (in μm^{-1}) for the single-harmonic grating with h_1 = 20 nm (h_2 = 0), with c standing for the speed of light in vacuum. One can observe the existence of an ω-gap between 7.3 and 7.8 μm^{-1}. For simplicity, we have neglected the dispersion of the media. The values of the intensity for $k_x > 1.5\,\omega/c$ can be larger than unity, because this region corresponds to angles of incidence larger than 90°, taking into account that the refractive index of the cladding is equal to 1.5. The working wavelength has been fixed in the previous sections to 0.85 μm, and is presented by the horizontal dashed purple line. It lies at the lower boundary of the forbidden gap that is formed due to the interaction between the plasmons, propagating in the opposite direction on the substrate-metal interface. The real parts of their constants of propagation are superposed on the figure (blue thick lines). The corresponding imaginary parts are presented in Fig. 12b. When the real parts of the constants of propagation approach each other (with increasing ω), the interaction leads to a sharp increase of the imaginary part, leading to a formation of the band gap. Further increase of ω leads to a separation of the propagation constants, a decrease of the imaginary part, and a creation of the upper propagation region.

The increase of the imaginary parts at around 7.3 μm^{-1} is accompanied by a slight curvature of the real parts and is due to the interaction between the plasmon surface waves propagating on the upper and lower surfaces of the metallic layer.

#96429 - $15.00 USD Received 20 May 2008; revised 14 Jul 2008; accepted 16 Jul 2008; published 21 Jul 2008
(C) 2008 OSA

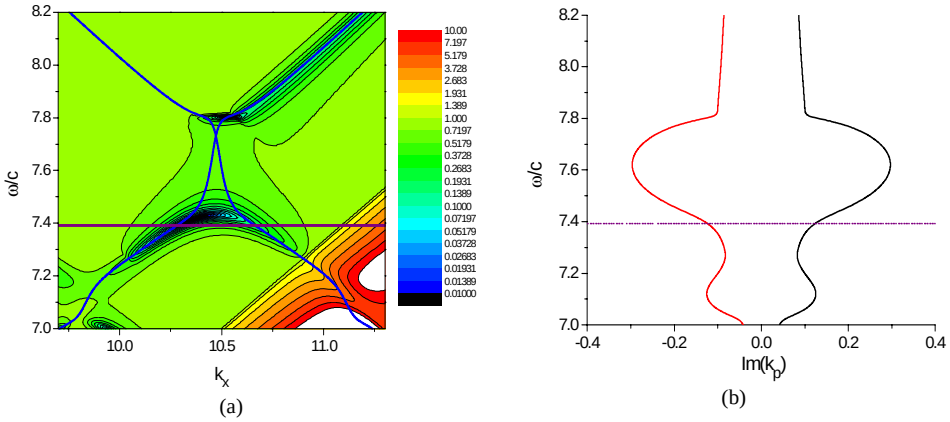

Fig. 12. (a) Colour map dependence of the intensity of the 0th reflected order of a single-harmonic grating with h_1 = 20 nm (h_2 = 0). Thick blue lines, real part of the constant of propagation of the plasmon surface waves excited on the substrate-metal layer interface. Purple line, working point at λ = 0.85 μm. (b) Imaginary parts of the surface wave propagation constants as a function of ω/c.

Figure 13 represents results similar to Fig. 12, but for the grating having two Fourier harmonics. There are several important differences. First, the second Fourier harmonic, which is responsible for the direct coupling between the two counter-propagating surface waves leads to a significant lowering of the boundaries of the forbidden zone, which extends in this case from 6.8 to 7.3 μm^{-1} in ω/c. Second, the imaginary parts of the propagation constants are larger than in the single-harmonic case. As a result, the working point is shifted from the lower to the upper boundary of the forbidden gap. As observed in Fig. 13a, the upper boundary is flatter than the lower one, so that one can expect stronger sensitivity with respect to the substrate refractive index, which is the case, as shown previously.

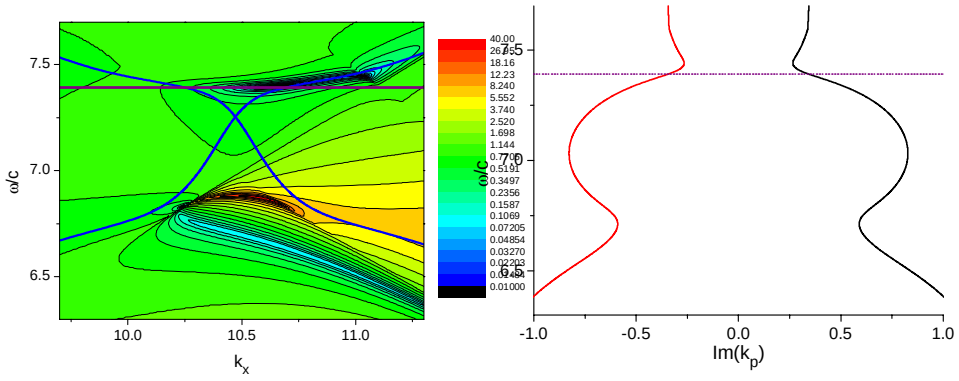

Fig. 13. Same as in Fig. 12, but for a double-harmonic grating with h_1 = 35 nm, h_2 = 59 nm, and $\varphi = \pi/2$.

#96429 - $15.00 USD Received 20 May 2008; revised 14 Jul 2008; accepted 16 Jul 2008; published 21 Jul 2008
(C) 2008 OSA

5. Conclusion

We have shown that the optimization of sensitivity of grating SPR sensors can be carried out on the basis of an understanding of the trajectories of zeros and poles of the scattering matrix. We have also shown that the use of gratings having two Fourier components can yield significantly improved sensitivity over the simple sinusoidal profile. In addition to increasing sensitivity, the reflectance curves can be optimized to have a single dip rather than the double-dip curve for the optimal sinusoid. Such simpler reflectance curves would be more amenable to an automated SPR analysis in large scale screening procedures for a range of biomolecules.

The sinusoidal and composite sinusoidal profiles investigated here are of the type amenable to holographic interference production. We plan to extend our investigations to step profiles, of the type more readily produced by lithographic or ion beam techniques.

Acknowledgments

Ross McPhedran acknowledges support from the Australian Research Council's Discovery Projects Scheme. His work on this project was also supported by the C.N.R.S., France.

#96429 - $15.00 USD Received 20 May 2008; revised 14 Jul 2008; accepted 16 Jul 2008; published 21 Jul 2008
(C) 2008 OSA